NÖHÜ Müh. Bilim. Derg. / NOHU J. Eng. Sci., 2024; 13(4), 1074-1079

Niğde Ömer Halisdemir Üniversitesi Mühendislik Bilimleri Dergisi
Niğde Ömer Halisdemir University Journal of Engineering Sciences

Araştırma makalesi / Research article

www.dergipark.org.tr/tr/pub/ngumuh / www.dergipark.org.tr/en/pub/ngumuh

Fabrication and analysis of ZnO and Al-doped ZnO films using the SILAR technique

ZnO ve Al-katkılı ZnO filmlerin SILAR tekniğiyle üretimi ve analizleri

İlker Kara[1,*], Abjar Ibrahim Rashid Hafedh[2], Ihsan Sadeq Raheem Waeli[3]

[1] *Çankırı Karatekin University, Graduate School of Natural and Applied Sciences, 18100 Çankırı, Türkiye*

Abstract

In this study, pure ZnO and Al-doped ZnO thin films at different concentrations were successfully grown on an ITO substrate using the SILAR method. The produced thin films were characterized by SEM/EDS, XRD, and UV-Vis spectroscopy. According to the XRD analysis results, it was observed that the produced thin films crystallized on a nanometer scale, and the crystallization quality varied depending on the concentration of Al doping. SEM/EDS analysis results indicated that Al-doped ZnO thin films affected the morphology, forming nano-root structures. UV-Vis analysis results showed that the band gap values of the thin films produced varied depending on the Al dopant, with decreased values, sharper absorption edges, and increased absorption intensities.

Anahtar kelimeler: SILAR metot, Çinko oksit, Al katkılı ZnO

Öz

Bu çalışmada, farklı konsantrasyonlarda saf ZnO (Çinko Oksit) ve Al-katkılı ZnO ince filmler, ITO tabanı üzerine SILAR yöntemi ile başarıyla büyütüldü. Üretilen ince filmler SEM/EDS, XRD ve UV-Vis spektroskopisi ile karakterize e*dilmiştir.* XRD analizi sonuçlarına göre, üretilen ince filmlerin nanometre ölçeğinde kristalleştiği ve kristalleşme kalitesinin Al-katkı konsantrasyonuna bağlı olarak değiştiği gözlendi. SEM/EDS analizi sonuçları, Al-katkılı ZnO ince filmlerin morfolojisi üzerinde etkilemiş olup nano-kök yapılar oluştur*ulmuştur.* UV-Vis analizi sonuçları, Al-katkı maddesine bağlı olarak üretilen ince filmlerin yasak enerji aralığı değerleri azalmış, soğurma kenarının keskinleştiği ve soğurma yoğunluğunun arttığı gözlendi.

Keywords: SILAR method, Zinc oxide, Al doped ZnO

1 Introduction

In recent years, the development of functional materials for various technological applications has garnered significant interest among researchers [1-3]. ZnO thin films, in particular, have emerged as promising candidates for diverse applications due to their unique properties, including wide bandgap, high electron mobility, and transparency in the visible region [3-5]. ZnO thin films are renowned for their wide bandgap, high electron mobility, optical transparency, and remarkable piezoelectric properties, rendering them indispensable in numerous cutting-edge technologies [6]. The incorporation of dopant elements such as aluminum (Al) into ZnO thin films further enhances their functionalities, leading to tailored material properties suitable for specific applications [7].

ZnO thin films hold a pivotal position in diverse technological applications owing to their unique optical and electronic properties [8,9]. These properties, including a wide bandgap and high electron mobility, render them indispensable in various optoelectronic devices such as solar cells, light-emitting diodes (LEDs), lasers, and sensors [10]. Additionally, ZnO thin films exhibit excellent transparency in the visible spectrum and mechanical robustness, making them ideal candidates for transparent and flexible electronics, including touchscreens and smart windows [11]. Moreover, their potential in environmental and biomedical applications, such as gas sensing and bioelectronics, further underscores their significance in contemporary research and industry.

The fabrication of ZnO thin films requires careful consideration of growth techniques to achieve the desired film properties. Among these techniques, Physical Vapor Deposition (PVD), Chemical Vapor Deposition (CVD), and solution-based methods such as the Sequential Ionic Layer Adsorption and Reaction (SILAR) technique stand out [12]. Each technique offers distinct advantages and challenges, influencing its suitability for specific applications and film characteristics [13]. For instance, PVD techniques ensure precise control over film thickness and composition, while solution-based methods like SILAR offer cost-effective and scalable approaches for large-scale production.

The application areas of ZnO compound encompass a wide array of fields. Among the most commonly preferred application areas are gas sensors, photodetectors, solar cells, light-emitting devices (LEDs), and laser systems [14]. Additionally, permeable ZnO thin films doped with elements such as aluminum and gallium exhibit excellent electrical conductivity [15].

The addition of Aluminium induces significant alterations in the electrical and optical characteristics of ZnO thin films. Notably, the electrical resistivity of all films increases with radiation dose. Moreover, the annealing environment during thin film production exerts a notable

* Sorumlu yazar / Corresponding author, e-posta / e-mail: karaikab@gmail.com (I. Kara)
Geliş / Recieved: 18.02.2024 Kabul / Accepted: 06.05.2024 Yayımlanma / Published: 15.10.2024
doi: 10.28948/ngumuh.1439098

influence on both electrical and optical properties. The annealing process has a more significant impact on these properties compared to ambient conditions and the increase in the Al additive ratio. [16]. The study highlights that Al doping leads to substantial variations in the electrical properties of ZnO thin films. Furthermore, the optical transmittance behavior underscores a blue-shift in the absorption edge, resulting in heightened electrical resistance and electron trapping rather than oxygen atom vacancies [16].

$$ZnCl_2 + 2NH_4OH \leftrightarrow Zn(OH)_2 + 2NH_4^+ + 2Cl^- \quad (1)$$

$$Zn(OH)_2 + 4NH_4^+ \leftrightarrow [Zn(NH_3)_4]^{2+} + 2H_2O + 2H^+ \quad (2)$$

$$[Zn(NH_3)_4]^{2+} + 4H_2O \rightarrow Zn(OH)_2\,(s) + 4NH_4^+ + 2OH^- \quad (3)$$

In the study conducted, it was observed that the particle sizes of Al-doped ZnO thin films increased [17]. Additionally, the energy band gaps of the resulting thin films were narrowed with the introduction of Al. Furthermore, it was concluded that the onset of absorption shifted towards longer wavelengths as a result of Al doping.

It was noted that the absorption edge experienced a blue shift with the intensification of Al doping in ZnO thin films. Additionally, the permeability demonstrated a decrease with the escalation of annealing temperature. This phenomenon of the absorption edge is referred to as the Burstein-Moss Effect [18].

In this context, this study aims to explore and elucidate the growth mechanisms and properties of undoped ZnO and Al-ZnO thin films deposited via the SILAR method. Through comprehensive characterization using techniques such as SEM, XRD, and UV-vis, insights into the influence of Al doping concentration on the structural and optical properties of ZnO thin films will be gained. The findings of this study are expected to contribute to the optimization of growth processes and the design of ZnO-based materials for advanced technological applications.

2 Materials and methods

The Sequential Ionic Layer Adsorption and Reaction (SILAR) method stands out as a versatile and cost-effective approach for thin film fabrication [3]. Widely utilized across scientific research and various disciplines, including materials science, solar cells, sensors, and optoelectronic devices, SILAR offers a straightforward and accessible means to precisely control thin film growth and tailor their properties. In this thesis study, the SILAR method was chosen for the fabrication of both undoped ZnO films and ZnO films doped with Al due to its suitability and effectiveness in achieving the desired film characteristics.

2.1 Preparation of substrate materials

In this study, thin films of undoped ZnO, as well as ZnO doped with Sn and Cu, were deposited onto ITO substrates. The ITO-coated glass substrates used were of the TEC8 model, measuring 25 mm x 25 mm with a thickness of 2 mm. Prior to deposition, the ITO-coated glasses underwent a thorough cleaning process. Initially, they were rinsed in a soapy water solution to remove any surface contaminants. Subsequently, the glass substrates with ITO coatings were subjected to ultrasonic cleaning using acetone for a duration of ten minutes. Following this, they were further cleaned with ultrasonication in a 1:1 ethanol-water solution for an additional ten minutes.

2.1.1 Production process

The growth of ZnO thin films on the ITO substrate utilized the ($[Zn(NH_3)_4]^{2+}$) zinc-ammonia complex. To prepare this complex solution, a mixture of 0.1 M $ZnCl_2$ (pH≈5.5) and 25 - 28 % NH_3 solutions was combined in a 1 to 10 molar ratio [Zn:NH_3=1:10] (Figure 1). Chemical reactions occurring during the thin film growth phase are elucidated by Equations (1), (2), and (3) [8].

To fabricate films of Al-doped ZnO the ITO substrate underwent a thorough cleaning process. Subsequently, solutions were prepared according to the specified additive ratio. Utilizing the SILAR approach, thin films of zinc oxide (ZnO) doped with tin and copper were deposited onto the indium tin oxide (ITO) substrate.

Figure 1. Mechanism of growth of ZnO thin films on ITO substrate by SILAR technique

The research focused on investigating the structural, surface, and optical characteristics of ZnO and Al-doped ZnO films deposited on an ITO substrate. To characterize these attributes comprehensively, a range of imaging techniques was employed, including X-ray diffractometry, FESEM, UV-Vis, and current-voltage measurements. UV-Vis analyses provided absorbance and transmittance spectra, which were utilized to calculate the band structure and band gap energies of the films. XRD analyses were performed using an APD 2000 PRO XRD device to examine the crystallinity levels, half-peak widths, and Miller indices of the films.

3 Results and discussion

Al-doped ZnO samples, with doping concentrations of 1%, 2%, and 3%, were deposited using the SILAR method, involving 40 deposition cycles. Subsequently, the samples were subjected to annealing at 300 °C for 13 minutes.

Figure 2 shows the X-ray diffraction (XRD) analyses of the produced thin films, including (a) undoped ZnO, (b) ZnO with 1% Al doping, (c) ZnO with 2% Al doping, and (d) ZnO with 3% Al doping. The dominant diffraction peaks of

SnO:In(ITO) below, indicating the tetragonal crystal structure, are oriented in the (101) direction. It was observed that as the amount of Al additive increased, the peak intensities of the films increased while the half peak widths decreased. This suggests that the crystallization levels of the produced thin films vary depending on the Al additive ratio. Upon examination of the crystallization levels of the films, it was found that the ITO/ZnO/Al 3% film exhibited the best compatibility with the ITO layer.

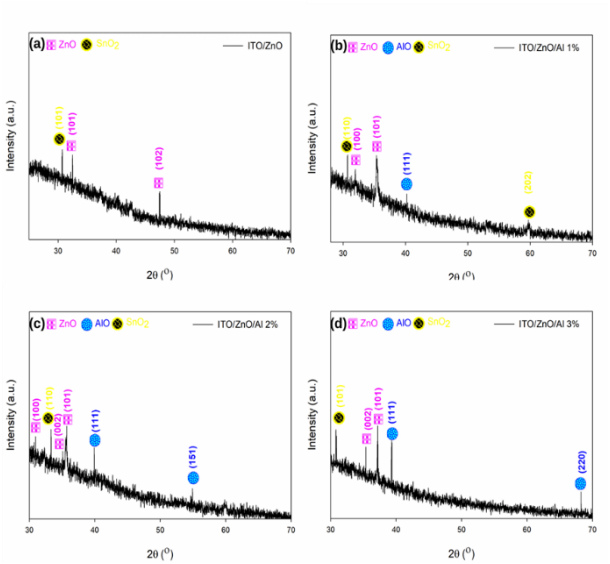

Figure 2. XRD analysis of produced (a) undoped ZnO, (b) ZnO 1% Al, (c) ZnO 2% Al, (d) ZnO 3% Al thin films

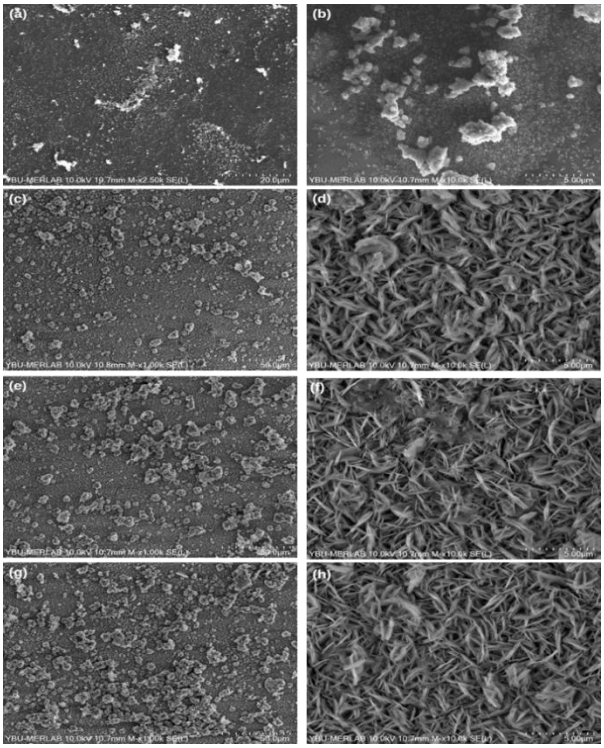

Figure 3. SEM images of produced (a, b) undoped ZnO, (c, d) ZnO 1% Al, (e, f) ZnO 2% Al, (g, h) ZnO 3% Al thin films

Sequential analyses were conducted on the thin films produced, with each doping ratio examined individually. Figure 3 presents scanning electron microscopy (SEM) images of both the undoped ZnO and Al-doped ZnO thin films, including 1%, 2%, and 3% doping levels.

It was observed that the Al (1%, 2%, 3%) doped ZnO thin film samples exhibited a more uniform tendency for aggregation on the ITO surface. The surface morphology was characterized by nano-root-shaped structures, with the prevalence of these structures increasing as the Al doping ratio rose. However, the average grain size was observed to decrease with a lower Al additive ratio. Upon comparing the SEM images of the produced thin film samples, it was evident that the nano-root structure of the 3% Al-doped sample was more pronounced, with a reduction in gaps within the structure. This led to an increase in surface roughness, a desirable feature in certain sensor applications. Particularly in gas sensor applications, high surface roughness is advantageous.

EDS measurements were conducted to analyze the elemental contribution and composition ratios of both the undoped ZnO and Al-doped ZnO thin films. Figure 4 shows the EDS images of these thin films, including undoped ZnO and Al doping levels of 1%, 2%, and 3%.

The EDS spectra of the thin films reveal the presence of Mg, Si, O, C, and Na elements. When analyzing the produced thin films using EDS, variations were observed in the ratios of Zn, O, C, and Al elements in the samples depending on the Al additive ratio. The presence of Si, Na, and C elements in the EDS analyses can be attributed to the ITO substrate material. Additionally, the presence of Mg is likely due to impurities introduced during the fabrication process.

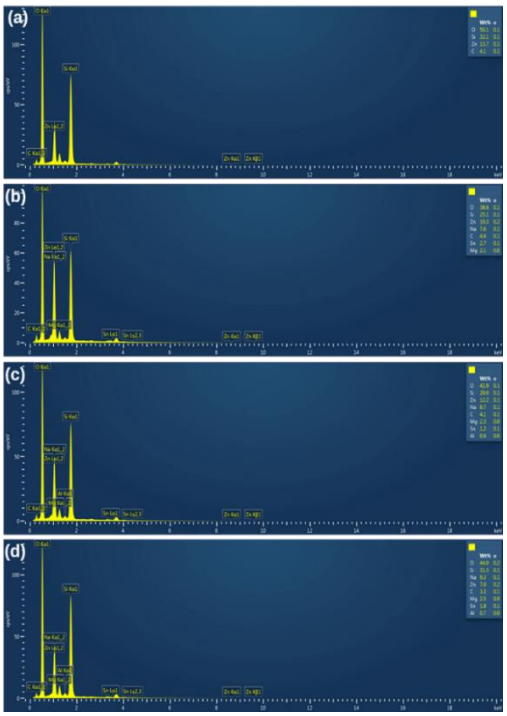

Figure 4. EDS images of produced (a) undoped ZnO, (b) ZnO 1% Al, (c) ZnO 2% Al, (d) ZnO 3% Al thin films

Figure 5 shows the absorption spectrum obtained from absorption measurements taken at room temperature for both undoped ZnO and Al-doped ZnO thin films fabricated using the SILAR technique. By utilizing the absorption measurements provided in Figure 5, the energy-dependent graph of $(\alpha hv)^2$ $(eVcm^{-1})^2$ was derived, as depicted in Figure 4.5.This figure showcases the forbidden energy gaps (E_g) of undoped ZnO and Al-doped ZnO thin films.

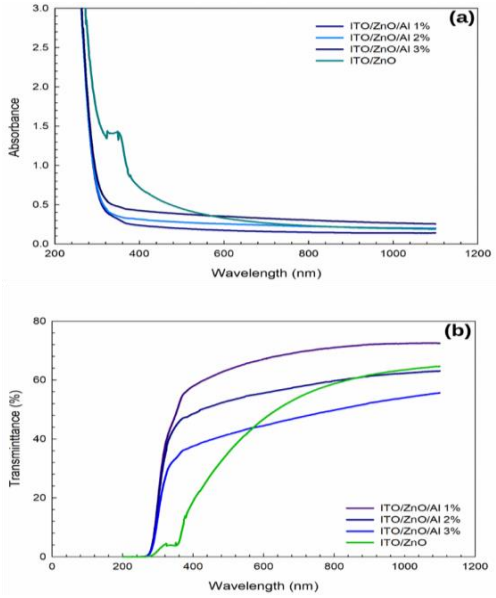

Figure 5. Energy dependent plots of $(\alpha hv)^2$ $(eVcm^{-1})^2$ plotted using optical absorption measurements of undoped ZnO and Al (1%, 2%, 3%) doped ZnO thin films (a) Absorbance, (b) Transmintance

Moreover, in Figure 6, the Urbach energy (E_u) was calculated from the slopes of the linear regions of (E_u) of $L_{n\alpha}$ to (hv). Table 1 below presents the E_g and E_u energies of the produced thin films corresponding to the Al additive ratio.

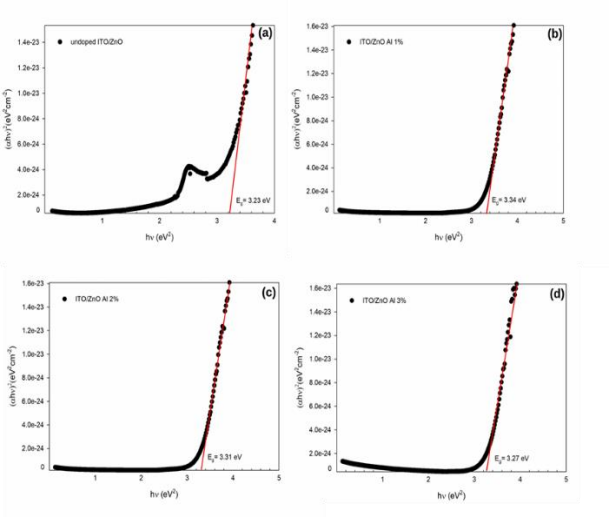

Figure 6. Graph of energy dependent forbidden band energy gap plotted using optical absorption measurements of thin films $(\alpha hv)^2$ $(eVcm^{-1})^2$

Table 1. Forbidden energy (E_g) and Urbach (E_u) values calculated from the energy dependent graphs of $(\alpha hv)^2$ $(eVcm^{-1})^2$ drawn using optical absorption measurements of undoped ZnO and Al (1%, 2%, 3%) doped ZnO thin films

Samples	E_g (eV)	E_u (meV)
Undoped ITO/ZnO	3.23	134.84
ITO/ZnO/Al 1 %	3.34	120.81
ITO/ZnO/Al 2 %	3.31	122.80
ITO/ZnO/Al 3 %	3.27	125.73

Table 1 presents the calculated forbidden energy values obtained from the $(\alpha hv)^2$ $(eVcm^{-1})^2$ energy graphs plotted using optical absorption measurements of undoped ITO/ZnO, as well as ITO/ZnO/Al (1%, 2%, 3%) doped ZnO thin films. It was observed that the forbidden energy gap values of the thin films, produced by incorporating Al into ZnO, varied depending on the doping level. Specifically, as the Al doping ratio increased, the forbidden energy gap values of the resulting thin films decreased. Additionally, it was noted that the absorption edge became sharper, while the absorption intensity increased.

This decrease in the forbidden energy gap value with respect to the Al-doping ratio can be attributed to the enhancement of crystallinity and surface properties of the produced thin films, along with an increase in grain size. According to Arif (2019), the particle sizes of Al-doped ZnO thin films were reported to increase. Furthermore, the energy band gaps of the resulting thin films narrowed with the inclusion of Al, leading to a shift in the onset of absorption towards longer wavelengths [18].

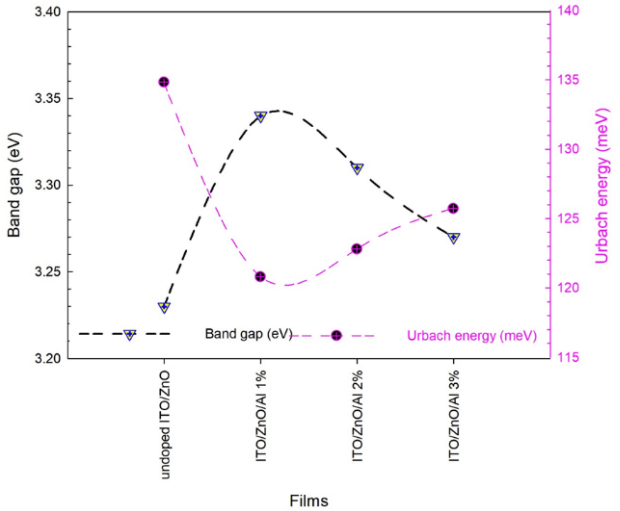

Figure 7. Band gap and Urbach energy graph of undoped ITO/ZnO, ITO/ZnO Al 1%, ITO/ZnO Al 2%, and ITO/ZnO 3% ZnO thin films

As seen in Table 1, a decrease in the forbidden energy gaps of the thin films was observed with an increase in the Al doping ratios of both undoped ITO/ZnO and ITO/ZnO/Al (1%, 2%, 3%) doped thin films. However, an increase in the Urbach energy (E_u) values was noted corresponding to the

Al additive ratio of the produced thin films. Figure 7 illustrates a decrease in Eg values and an increase in E_u values depending on the Al contribution ratio. It is expected that E_g decreases and E_u increases with Al-doping [19]. This observation aligns with the anticipated behavior where the band gap energy of Al-doped ZnO thin films is smaller than that of undoped ZnO thin films, attributed to the Burstein-Moss shift [19]. Furthermore, with an increasing Al-doping ratio, the Fermi energy level of ITO/ZnO/Al shifts towards the conduction band, leading to a decrease in the forbidden energy gap as illustrated in Figure 7.

4 Conclusion

In this study, undoped ITO/ZnO and Al (1%, 2%, 3%) doped ITO/ZnO thin films were fabricated on ITO substrates using the SILAR method. The primary objective of this study was to investigate the structural, morphological, and optical properties of both undoped ITO/ZnO and Al-doped ITO/ZnO thin films.

In XRD analysis, undoped ITO/ZnO and Al-doped ITO/ZnO thin films grown on ITO substrates showed increased peak intensities and decreased half-peak widths with rising Al-doping levels. Additionally, doped films exhibited decreased peak intensities and increased half-peak widths compared to undoped films.

SEM images of Al-doped ITO/ZnO samples revealed a nano-root structure, notably more pronounced in the 3% Al-doped ITO/ZnO sample. However, an increase in the Al additive ratio was associated with a decrease in the average grain size.

Upon examination of optical absorption measurements for Al (1%, 2%, 3%) doped ITO/ZnO thin films produced on ITO substrates, it was noted that the forbidden energy gap values of the films decreased with increasing Al-doping ratio. As the Al additive ratio increased, the forbidden energy gap values of the thin film samples decreased, leading to a sharper absorption edge and increased absorption intensity. This decrease in the forbidden energy gap of the produced thin films can be attributed to the improvement in film crystallinity and surface properties, as well as an increase in grain size.

Upon evaluating the results of the analyses conducted within the scope of the study, it was evident that alterations in the Al-doping ratios led to discernible modifications in the characteristic structure of the resulting thin films.

The results of this study can provide important contributions to practical applications. The increased particle sizes and decreased energy band gap of Al-doped ZnO thin films can be utilized in many potential applications such as solar cells, semiconductor devices, and optoelectronic components. Especially in materials science and engineering research and applications, Al-doped ZnO materials can be evaluated as a potential candidate.

Conflict of Interest

The authors declare that there is no conflict of interest.

Similarity rate (iThenticate): %20

References

[1] H. R. Khan, R. Akram, M. Aamir, M.A. Malik, A.A. Tahir, M.A. Choudhary, J. Akhtar. Investigations of photoelectrochemical performance of polycrystalline Bi-doped ZnO thin films. Journal of Physics and Chemistry of Solids, 181, 111529. https://doi.org/10.1016/j.jpcs.2023.111529.

[2] C. J. C. Singh, J. Samuel, C. S. Biju, S. S. J. Dhas, S. Usharani. Effect of Sn doping on the structural, photoluminescence, ultraviolet filtering and antibacterial activity of ZnO nanorods. Optical and Quantum Electronics, 55 (12), 1072, 2023.

[3] A. Kompa, B.L. Devi, U. Chaitra. Determination of optical constants of vacuum annealed ZnO thin films using Wemple Di Domenico model, Sellmier's model and Miller's generalized rules. Materials Chemistry and Physics, 299, 127507, 2023. https://doi.org/10.1016/j.matchemphys.2023.127507.

[4] J. M. Bian, X. M. Li, X. D. Gao, W. D. Yu, L. D. Chen. Deposition and electrical properties of N-In codoped p-type ZnO films by ultrasonic spray pyrolysis. Applied Physics Letters, 84 (4), 541-543, 2004. https://doi.org/10.1016/j.tsf.2023.139958.

[5] I. C. B. Rodriguez, B. El Filali, T. Torchynska, J. Douda, I. R. Ibarra. Optical and structural properties of Sn doped ZnO thin films synthesized by spray pyrolysis. MRS Advances, 8 (24), 1434-1437, 2023. https:// doi.org/10.1557/s43580-023-00673-4.

[6] P. Dhamodharan, C. Manoharan, Dhanapandian, S.M. Bououdina, S. Ramalingam. Preparation and characterization of spray deposited Sn-doped ZnO thin films onto ITO subtracts as photoanode in dye sensitized solar cell. Journal of Materials Science: Materials in Electronics, 26, 4830-4839, 2015. https://doi.org/10.10 07/s10854-015-2990-7.

[7] A. A. El-Fadl, G. A. Mohamad, A. B., Abd El-Moiz, M. Rashad. Optical constants of Zn1- xLixO films prepared by chemical bath deposition technique. Physica B: Condensed Matter, 366 (1-4), 44-54, 2005. https://doi. org/10.1016/j.physb.2005.05.019.

[8] E. Holmelund, J. Schou, S. Tougaard, N. B. Larsen. Pure and Sn-doped ZnO films produced by pulsed laser deposition. Applied surface science, 197, 467-471, 2002. https://doi.org/10.1016/S0169-4332(02)00367-7.

[9] B. Kadem, H.A. Banimuslem, A. Hassan, Modification of morphological and optical properties of ZnO thin film. Karbala International Journal of Modern Science, 3 (2): 103-110, 2017. https://doi.org/10.1016/j.kijoms.0 17.04.003.

[10] M. Mekhnache, A. Drici, L.S. Hamideche, H. Benzarouk, A. Amara, L. Cattin, M. Guerioune. Properties of ZnO thin films deposited on (glass, ITO and ZnO: Al) substrates. Superlattices and Microstructures, 49(5), 510-518, 2011. https://doi.org/10.1016/j.spmi.2011.02.002.

[11] P. Nunes, B. Fernandes, E. Fortunato, P. Vilarinho, R. Martins. Performances presented by zinc oxide thin films deposited by spray pyrolysis. Thin Solid Films, 337 (1-2), 176-179, 1999. https://doi.org/10.1016/S0040-6090(98)01394-7.

[12] G. K. Paul, S.K. Sen, Sol-gel preparation, characterization and studies on electrical and thermoelectrical properties of gallium doped zinc oxide films. Materials letters, 57 (3), 742-746, 2002. https://doi.org/10.1016/S0167-577X(02)00865-0.

[13] S. T. Shishiyanu, T. S. Shishiyanu, O. I. Lupan. Sensing characteristics of tin-doped ZnO thin films as NO_2 gas sensor. Sensors and Actuators B: Chemical, 107 (1), 379-386, 2005. https://doi.org/10.1016/j.snb.2004.10.030.

[14] M. R. Vaezi, S. K. Sadrnezhaad. Improving the electrical conductance of chemically deposited zinc oxide thin films by Sn dopant. Materials Science and Engineering: B, 141 (1-2), 23-27, 2007. https://doi.org/10.1016/j.mseb.2007.05.010.

[15] D. Bao, H. Gu, A. Kuang. Sol-gel-derived c-axis oriented ZnO thin films. Thin solid films, 312 (1-2): 37-39, 1998. https://doi.org/10.1016/S0040-6090(97)00302-7

[16] G. Valle, P. Hammer, S.H. Pulcinelli, C.V. Santilli. Transparent and conductive ZnO: Al thin films prepared by sol-gel dip-coating. Journal of the European Ceramic Society, 24 (6): 1009-1013, 2004. https://doi.org/10.10 16/S0955-2219(03)00597-1.

[17] D. Baydoğan, A.B. Tuğrul. Evaluation of the optical changes for a soda-lime-silicate glass exposed to radiation. Glass Physics and Chemistry, 32: 309-314, 2006. https://doi.org/10.1134/S1087659606030096

[18] M. Arif, M. Shkir, S. AlFaify, V. Ganesh, A. Sanger, H. Algarni, A. Singh. A structural, morphological, linear, and nonlinear optical spectroscopic studies of nanostructured Al-doped ZnO thin films: An effect of Al concentrations. Journal of Materials Research, 34 (8), 1309-1317, 2019. https://doi.org/10.1557/jmr.2018.506.

[19] M. Thambidurai, J. Y. Kim, C. M. Kang, N. Muthukumarasamy, H. J. Song, J. Song, C. Lee. Enhanced photovoltaic performance of inverted organic solar cells with In-doped ZnO as an electron extraction layer. Renewable Energy, 66, 433-442, 2014. https:// doi.org/10.1016/j.renene.2013.12.031.